

# Study of the Evaporation of Pollutant Liquids under the Influence of Surfactants

Dimitrios Gavril, Khan Rashid Atta, and George Karaiskakis

Laboratory of Physical Chemistry, Dept. of Chemistry, University of Patras, 26504, Patras, Greece

DOI 10.1002/aic.10875

Published online April 26, 2006 in Wiley InterScience (www.interscience.wiley.com).

*In the present work, reversed-flow gas chromatography (RF-GC) is utilized for the study of the evaporation of volatile liquids. Evaporation rates and the respective diffusion coefficients are determined for the evaporation of ethanol and 1,1,1-trichloroethane in nitrogen, at 306.2 K. The precision (>99.5%) and accuracy of the method, as well as the uncertainty of the determined parameters, ascertain the potential of the presented methodology. The experimentally obtained evaporation rates have units of velocity, and for high volatility compounds their values are identified with the liquid film mass-transfer coefficients. The latter compare successfully to available literature values, further ascertaining the validity of the presented methodology. The variation of the evaporation rates of ethanol and 1,1,1-trichloroethane, in the presence of various amounts of Triton X-100, indicates that different, but in any case high amounts of surfactant are required for the drastic retardation of the vaporization rate. The reduction of the evaporation rate can be attributed either to the formation of densely packed surface monolayers or to the formation of an insoluble monolayer. © 2006 American Institute of Chemical Engineers AICHE J, 52: 2381–2390, 2006*

**Keywords:** evaporation, inverse gas chromatography, surfactants, ethanol, 1,1,1-trichloroethane, Triton X-100

## Introduction

Transport of chemicals from water bodies to the atmosphere (volatilization or evaporation) can be an important environmental pathway for certain chemicals. Evaporation is an important environmental fate for compounds introduced into both freshwater and marine environments by inadvertent spills, by agricultural runoff, and by industrial effluents, or introduced directly into the air from industrial unit processes such as bioreactors and cooling towers.<sup>1–7</sup>

Several groups have reported various methods for estimating volatilization or evaporation rates of organic chemicals from natural water bodies.<sup>1,4–7</sup> The methods described in the literature for the measurement of evaporation rates can be classified in two main classes. The first involves the measurement of

weight gain of a vapor adsorbent placed above the liquid surface. This method allows relative rates across a quiescent gas space. The second class involves measurement of the rate of liquid loss into a gas stream flowing horizontally across the liquid surface. In the majority of these techniques relative evaporation rates,<sup>8</sup> which cannot be related to the physical properties of the evaporating species, as well as evaporation halftimes are measured.<sup>1,5,6</sup>

The novel technique of reversed-flow gas chromatography (RF-GC) has been used for various physicochemical measurements, such as of rate coefficients and diffusion coefficients for the evaporation of pure liquids,<sup>9</sup> mass transfer coefficients regarding the evaporation of liquids,<sup>10</sup> activity coefficients, and mass transfer coefficients and diffusion coefficients in multi-component liquid mixtures,<sup>11</sup> as well as for the estimation of the solubility and interaction parameters in binary liquid mixtures.<sup>12</sup>

Certain monolayers have been found to cause a significant reduction in the evaporation rate of a liquid; for example, long

Correspondence concerning this article should be addressed to D. Gavril at D.Gavril@upatras.gr.

chain alcohols decrease the volatilization rate of the water on an actual lake by a factor of 46-50%.<sup>13-19</sup>

In the present work, the utilization of RF-GC is extended in the study of the evaporation of two volatile organic compounds, that is 1,1,1-trichloroethane and ethanol, under the influence of the liquid free surface area as well as under various amounts of the nonionic surfactant Triton X-100.

## Methods

### Preparation of the surfactant-containing solutions

In order to prepare the various surfactant+solvent solutions, the amount of the surfactant adsorbed per unit area of interphase was calculated by using the appropriate form of the Gibbs adsorption equation (for solutions of nonionic surfactants)<sup>20</sup>

$$\Gamma_1 = -\frac{1}{2.303RT} \left( \frac{\partial \gamma}{\partial \log C_1} \right)_T \quad (1)$$

where  $\gamma$  is the surface tension in  $\text{N}\cdot\text{m}^{-1}$  or  $\text{J}\cdot\text{m}^{-2}$ ,  $C_1$  is the molar concentration of the surfactant at the experimental absolute temperature  $T = 298.2 \text{ K}$ ,  $R = 8.314 \text{ J}\cdot\text{mol}^{-1}\text{K}^{-1}$  is the ideal gas constant, and  $\Gamma_1$  is the surface excess concentration of the surfactant in  $\text{mol}\cdot\text{m}^{-2}$ . In order to estimate the surface area per molecule,  $\alpha_1^s$ , of Triton X-100 at the interphase, the surface tension ( $\gamma$ ) was plotted against the log of the concentration ( $C_1$ ) of Triton X-100, as shown in Figure 1.

From the slope of Figure 1, the surface excess concentration of the surfactant was determined:  $\Gamma_1 = (2.67 \pm 0.07) \cdot 10^{-6} \text{ mol}\cdot\text{m}^{-2}$ . Using the  $\Gamma_1$  value so obtained, specific surface area per molecule at the interphase,  $\alpha_1^s$ , was calculated from the following relation<sup>20</sup>:

$$\alpha_1^s = \frac{10^{20}}{N_A \Gamma_1} \quad (2)$$

where  $N_A$  is the Avogadro's number and  $\Gamma_1$  is in  $\text{mol}\cdot\text{m}^{-2}$ . It was found that  $\alpha_1^s = (62.294 \pm 0.002) \cdot 10^{-10} \text{ m}^2$ . Both  $\Gamma_1$  and

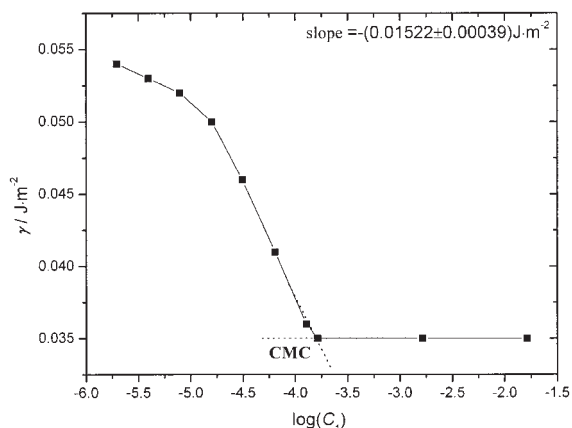


**Figure 1.** Plot of the surface tension ( $\gamma / \text{J}\cdot\text{m}^{-2}$ ) against the log of  $C_1$ , where  $C_1$  is the bulk phase concentration of the various aqueous solutions of surfactant Triton X-100, at 25°C.

CMC = Critical micelle concentration of surfactant.

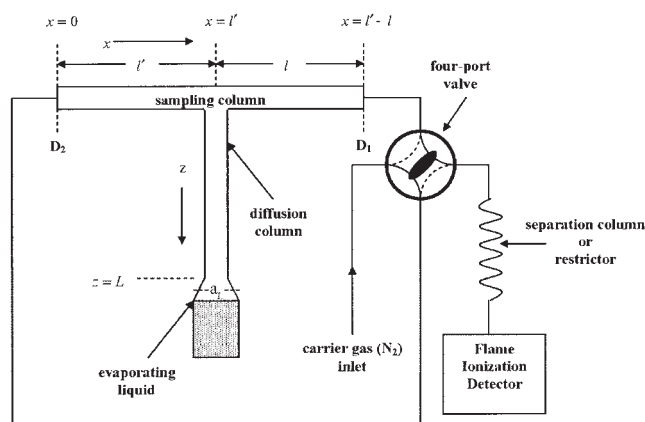


**Figure 2.** Instrumentation of the reversed-flow gas chromatography technique for the simultaneous measurement of diffusion coefficients and rate transfer coefficients of evaporating liquids.

$\alpha_1^s$  values are of the same order of magnitude with the values given on page 78 of Ref. 20 for similar nonionic compounds of homogeneous head group.

For the aqueous solutions of Triton X-100 used in the surface tension experiments, the critical micelle concentration was found to be  $C_1 = 1.56 \cdot 10^{-4} \text{ M}$  or 0.0094% vol. Since both the surface area of the bottle containing the evaporating liquid under study,  $a_L$ , as well as the specific surface area per molecule at the interphase,  $\alpha_1^s$  are known, the amount of surfactant compatible with the theoretical coverage ranging from 1 to 4 monolayers of Triton X-100 was estimated, and the respective solutions of surfactant in ethanol and in 1,1,1-trichloroethane were prepared.

## Materials

1,1,1-trichloroethane and ethanol from MERCK-Schuchardt, England, were used as evaporating liquids (stationary phase).

Nonionic surfactant Triton X-100 (iso-Octylphenoxypolyethoxyethanol,  $d = 1.06 \text{ g}\cdot\text{ml}^{-1}$  and  $M = 646.37 \text{ g}\cdot\text{mol}^{-1}$ ) was equipped from BDH Laboratory Supplies, England. Nonionic surfactants are compatible with all other types of surfactants, and they are soluble in water and organic solvents including hydrocarbons. Triton X-100 is more soluble than other non-ionic surface active agents and ~90% biodegradable.

Nitrogen of 99.999% purity from BOC Gases, Athens, Greece, was used as the carrier-gas (mobile phase).

## Techniques

In RF-GC, another column (diffusion column) is placed perpendicularly in the center of the usual chromatographic column (sampling column), as shown in Figure 2. The carrier gas flows continuously through the sampling column  $l + l'$ , while it is stagnant inside the diffusion column  $L$ . The evaporating liquid (stationary phase) is placed into a glass bottle at the lower closed end of the diffusion column.

In contrast with conventional GC, where the mobile phase is the center of interest, in RF-GC the solid or liquid substance placed into the closed end of the diffusion column is under investigation. Thus, RF-GC can be considered as an inverse gas

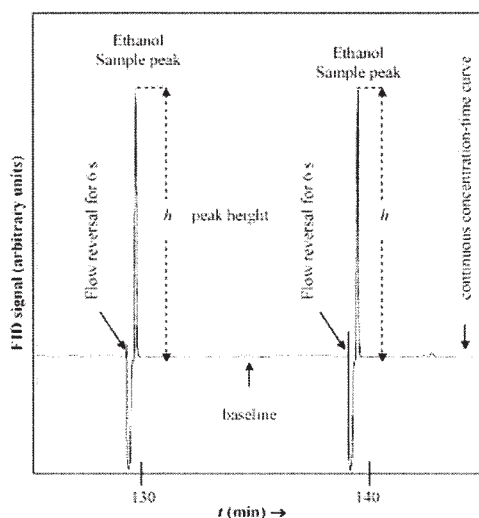


**Figure 3. A reversed-flow chromatogram showing two sample peaks for the diffusion of ethanol vapors into carrier gas nitrogen at 306.2 K and 101325 Pa (volumetric flow rate =  $60 \text{ cm}^3 \cdot \text{min}^{-1}$ ).**

chromatographic method. Column sections  $l + l'$  form the so-called sampling column, at which junction with the diffusion column  $L$ , the sampling of the physicochemical phenomena taking place into the diffusion column  $L$  is done. In our case, the physicochemical phenomena occurring into the diffusion column are: (a) the evaporation of small amounts of the studied liquid solvents, and (b) the diffusion of the evaporating vapors into the stagnant carrier gas. Consequently, the displacement of the vapors of the evaporating liquid into the diffusion column depends on the properties of the stationary phase and the diffusion of its vapors into the stagnant carrier gas (mobile phase), while it is independent of carrier gas flow-rate.

Another feature of RF-GC is the sampling procedure of the physicochemical phenomena, which take place in the diffusion column. The sampling procedure is carried out by using a four-port valve enabling reversals of the flow of the carrier gas for a short time, as well as restoring its flow in its original direction. The above-mentioned flow reversal procedure results in a brief enrichment of the solute quantity into the carrier gas and, thus, extra chromatographic peaks, like those of Figure 3, are created on the continuous concentration-time curve (chromatogram). The extra peaks are symmetrical and their height (or the area) measured from the continuous baseline is proportional to the concentration of the diffusing vapors of the liquid stationary phase at the junction of the diffusion and sampling columns, giving to RF-GC a higher sensitivity and accuracy, resulting in accurate data collection and limiting the need for computer data reduction that seems necessary for other elution methods.

Surface tension measurements were performed by using a Torsion Balance from White Elec. Inst. Co. Ltd.

### Procedure

The experimental setup for the application of reversed-flow gas chromatography to study the evaporation is shown in

Figure 2, the details of which have been described elsewhere,<sup>9,21,22</sup> except that the system was modified for the periodic flow reversal of the carrier gas with an automatic Shimadzu four-port valve. The computer programming during the whole experiment controlled the flow reversals.

A multi-detector gas chromatograph (Shimadzu GC-14 A), equipped with a flame ionization detector along with other detectors, contained in its oven two sections of length  $l$  and  $l'$  of the stainless-steel sampling column  $l + l'$  [(50 + 50) cm  $\times$  5.3 mm i.d.], which were empty of any chromatographic material. A stainless-steel diffusion column, having length  $L = 45$  cm (Figure 2), was connected perpendicularly in the middle of the sampling column. The glass bottle containing the liquid stationary phase was connected at the lower end of the diffusion column,  $L$ , with a  $\frac{1}{4}$  inch stainless steel tee. The ends  $D_1$  and  $D_2$  of the sampling column  $l + l'$  were connected with the carrier gas inlet and the flame ionization detector via an automatic four-port Shimadzu valve.

After placing the liquid under study in its position, the automatic valve was regulated in such a way that as soon as the monotonously rising concentration-time curve for the vapor of the liquid appeared on the monitor, the chromatographic sampling procedure started by reversing the flow of carrier gas for an exact time period of 6 s. This interval is a shorter time period than the gas hold-up time in both sections of  $l$  and  $l'$ . As soon as the carrier gas flow was restored in its original direction, sample peaks, like those in Figure 3, were recorded, corresponding to various times from the beginning of the experiment. The automatic procedure operates continuously at various time intervals, during the whole experiment lasting approximately 4 h.

All the experiments were performed at 306.2 K, under a flow rate equal to  $1.0 \text{ cm}^3 \cdot \text{s}^{-1}$ , while the pressure drop along the system was negligible. The volume of the glass bottle containing the evaporating liquids was  $4.0 \text{ cm}^3$  and the height of the liquid substance into the bottle was 1.0 cm.

### Study of the evaporation under the influence of the liquid surface area and surfactant monolayers

The influence of the liquid free surface area on the evaporation of 1,1,1-trichloroethane and ethanol was studied by using four different surface area,  $a_L$ , glass bottles, which contained the evaporating liquids, at a fixed temperature of 306.2 K and pressure of 101325 Pa. The four bottles used in these experiments were: 0.613, 2.333, 4.250, and  $4.677 \cdot 10^{-5} \text{ m}^2$ , respectively.

Five different experiments were performed for each studied liquid, starting from pure liquid and subsequently under the influence of 1-4 theoretical monolayer(s) of Triton X-100, on a glass bottle of surface area,  $a_L$ , equal to  $4.250 \cdot 10^{-5} \text{ m}^2$ , at 306.2 K and pressure of 101325 Pa.

## Theoretical Basis

### Mathematical model

The variation of the sampling peaks height as a function of time  $t_0$ , for the vaporization of ethanol into nitrogen at 306.2 K, is shown in Figure 4. A steep rise and then leveling off with time of the sample peak height is observed, as is expected for the process of the evaporation.<sup>18</sup>

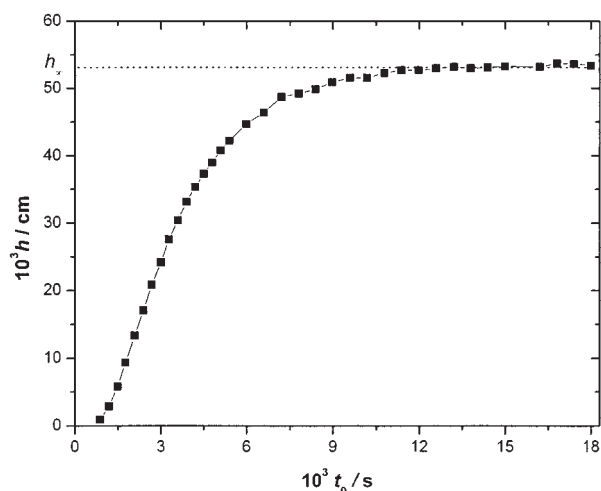


**Figure 4. Diffusion band (plot of sample peaks height,  $h$ , against time,  $t_0$ , from the beginning of the experiment) for the volatilization of ethanol, at 306.2 K and 101325 Pa.**

$h_\infty$  is the infinity value of the sample peak height, taken as the mean of the values found in the long time interval.

It has been shown earlier that each sample peak, produced by two successive reversals in RF-GC, is symmetrical and its maximum height  $h$  from the ending baseline is given by<sup>9</sup>:

$$h \cong 2c(l', t_0) \quad (3)$$

Thus, the concentration of the vapors of an evaporating liquid,  $c(l', t_0)$ , at  $x = l'$  and time  $t_0$  is proportional to the height or the area of the experimentally obtained sampling peaks, and it is interrelated with the rate coefficient for the evaporation process,  $k_c$ , the diffusion coefficient of the vapor into the carrier gas,  $D$ , and the geometrical details of the diffusion column through the relation<sup>9</sup>:

$$c(l', t_0) = \frac{k_c D c_0}{\nu(k_c L + D)} \{1 - \exp[-2(k_c L + D)t_0/L^2]\} \quad (4)$$

where  $L$  is the length of the diffusion column and  $\nu$  the volumetric flow rate of the carrier-gas. Figure 4 represents the sampling of the above-mentioned processes against time. It becomes obvious that after a period of time, which is characteristic of each particular interaction system, a steady-state situation is achieved. From this plot, at long times an infinite value for the peak height  $h_\infty$  can be obtained. This infinity  $h_\infty$  value is used for the linearization of the resulting relation<sup>9</sup>:

$$h_\infty = 2k_c D c_0 / [\nu(k_c L + D)] \quad (5)$$

Using the former approximation, one obtains<sup>9</sup>:

$$\ln(h_\infty - h) = \ln h_\infty - [2(k_c L + D)/L^2]t_0 \quad (6)$$

Thus, at long enough times, for which Eq. 4 was derived, a plot of  $\ln(h_\infty - h)$  vs.  $t_0$  is expected to be linear, and from its slope

$-2(k_c L + D)/L^2$  a first value of  $k_c$  can be calculated from the known value of  $L$  and a literature or theoretically calculated value of  $D$ .<sup>23-25</sup>

The value of  $k_c$  can now be used to plot small-time data according to Eq. 14 of Ref. 9, which is substituted now for  $c(l', t_0)$  in Eq. 2. After rearrangement logarithms are taken, and there results:

$$\ln \left[ h \left( \frac{L}{2t_0^{1/2}} + k_c t_0^{1/2} \right) \right] = \ln \left[ \frac{4k_c c_0}{\nu} \left( \frac{DL}{\pi} \right)^{1/2} \right] - \frac{L^2}{4D} \frac{1}{t_0} \quad (7)$$

Now a plot of the lefthand side of this relation versus  $1/t_0$  will yield a first approximation experimental value for  $D$  from the slope  $-L^2/4D$  of this new linear plot.

### Calculations

The analysis of the experimental chromatographic findings is done from Eqs. 6 and 7 as follows. Leaving out the first 3-4 points, which correspond to small times, the rest of the experimental points are plotted according to Eq. 6. As infinity value  $h_\infty$  was taken, the mean of the values found in the time interval was 135-180 min. From the slope of this plot, using a theoretically calculated value of  $D$  (such as equal to  $1.32 \cdot 10^{-5} \text{ m}^2 \text{ s}^{-1}$  for the diffusion of ethanol in nitrogen) and the actual value of  $L$  (45.0 cm), a first value for  $k_c$  is calculated. The value of  $L$  is experimentally measured, while the value of  $D$  can be reliably determined either experimentally or predicted by theoretical approaches. Several empirical methods to estimate  $D$  for binary gas systems have been presented. The most widely used method is that of Fuller-Schettler-Giddings, which results from the correlation of more than 340 experimental diffusion coefficients for 153 different binary mixtures and combines simplicity and accuracy.<sup>25</sup> In a recent review article, the determination of diffusion coefficients by gas chromatography was demonstrated and evaluated.<sup>23</sup> In the same work, a big data base of literature  $D$  values is available.

The above  $k_c$  value is now used to plot all the points except those close to  $h_\infty$ , which correspond to long times, according to Eq. 7. From the slope of this latter plot, an experimental value for  $D$  is found. If this is combined with the slope of the previous plot, a second value for  $k_c$  is calculated and further used to re-plot the data according to Eq. 7. The new value for  $D$  found coincides with the previous one, and thus the iteration procedure can be stopped.

### Possible sources of errors

The uncertainty in the experimentally determined evaporation parameters mostly depends on the accuracy of the temperature control. The uncertainty in the sample temperature is  $\pm 0.1 \text{ K}$ . The main source of error in the determination of the diffusion coefficient is the accuracy with which the length of the diffusion column,  $L$ , is measured, since  $D$  is proportional to  $L^2$ . Instead of measuring  $L$  directly, one can use a solute of accurately known diffusion coefficient in the given carrier gas (such as  $\text{C}_2\text{H}_6$  in  $\text{N}_2$ <sup>23</sup>) and carry out a calibration experiment for  $L$ . The value of  $L$  so determined (45 cm) can now be used to estimate unknown diffusion coefficients. The determination



**Table 1. Rate Coefficients for the Evaporation of Ethanol,  $k_c$ , and Diffusion Coefficients of Its Vapors into Nitrogen,  $D_{\text{found}}$ , Under the Effect of Liquid Free Surface Area,  $a_L$ , at 306.2 K and 101325 Pa**

Vessel No	$10^5 a_L/\text{m}^2$	$10^5 k_c/\text{m s}^{-1}$	$10^5 D_{\text{found}}/\text{m}^2\text{s}^{-1}$	$10^5 D_{\text{lit}}/\text{m}^2\text{s}^{-1}$	$10^5 D_{\text{lit}}/\text{m}^2\text{s}^{-1}$	Deviation, %	Deviation, %
1	0.613	$4.70 \pm 0.13^a$	$1.30 \pm 0.006^a$	$1.32^\dagger$	$1.37^\ddagger$	$1.5^\dagger$	$5.1^\ddagger$
2	2.333	$5.34 \pm 0.15^a$	$1.32 \pm 0.008^a$	$1.32^\dagger$	$1.37^\ddagger$	$0^\dagger$	$3.6^\ddagger$
3	4.250	$6.32 \pm 0.17^a$	$1.32 \pm 0.009^a$	$1.32^\dagger$	$1.37^\ddagger$	$0^\dagger$	$3.6^\ddagger$
4	4.677	$6.86 \pm 0.14^a$	$1.33 \pm 0.007^a$	$1.32^\dagger$	$1.37^\ddagger$	$0.8^\dagger$	$2.9^\ddagger$
	Mean values		$1.32 \pm 0.006$			$(0.6^\dagger)^{**}$	$(3.8^\ddagger)^{**}$
	Precision, %		99.5*				

<sup>a</sup>Uncertainty obtained from the standard errors of the  $k_c$  and  $D$  values, estimated from the slopes of the linear plots of Eqs. 6 and 7, respectively.

\*Precision determined from the mean value and the standard error of the experimentally obtained diffusion coefficients.

\*\*Mean deviation of the experimental diffusion coefficients from the respective predicted<sup>†</sup> and experimental<sup>‡</sup> literature values,  $D_{\text{lit}}$ .

of the evaporation rate depends also on the accuracy of the length of the diffusion column,  $L$ .

## Results and Discussion

The evaporation of pure liquids as well as of liquid mixtures has been studied in the past utilizing RF-GC.<sup>9-12</sup> However, the evaporation in the presence of surfactants is a more complex process than that of a simple liquid mixture. For this reason a preliminary evaluation of the technique was done for the first time, by performing evaporation experiments under various liquid surface areas. It is well known that the rate of the evaporation of a liquid, at a fixed temperature, is expected to increase with rising liquid surface area, while the diffusivity of the liquid vapors is expected to be unaffected. From the above mentioned experiments, the precision and the accuracy of the methodology can be determined by utilizing the experimentally obtained by means of RF-GC diffusion coefficients of the vapors of the evaporating liquid into the carrier gas (nitrogen). The reason for the use of diffusivities is that accurate diffusion coefficient data are more accessible in the literature, in contrast with evaporation data, for which relative evaporation rates and evaporation halftimes are usually found in the literature.

Several groups have reported various methods for estimating evaporation rates. The volatilization rate constant expressed in terms of the mass-transfer rates of a solute obeying Henry's law, across liquid-, gas- and surfactant-layer phase boundaries, according to the classical two-film mass transfer model<sup>26</sup> is<sup>8</sup>:

$$k_c = \frac{V k_v}{a_L} = \left[ \frac{1}{k_1} + \frac{RT}{H_c k_s} + \frac{RT}{H_c k_g} \right]^{-1} \quad (8)$$

where  $k_c$  is the experimentally obtained volatilization rate of the present work ( $\text{cm s}^{-1}$ ),  $k_v$  is the volatilization rate constant ( $\text{s}^{-1}$ ),  $a_L$  is the interfacial area ( $\text{cm}^2$ ),  $V$  is the liquid volume

( $\text{cm}^3$ ),  $k_1$  is the liquid-film mass-transfer coefficient ( $\text{cm s}^{-1}$ ),  $R$  is the gas constant ( $\text{J K}^{-1} \text{mol}^{-1}$ ),  $T$  is the temperature (K),  $H_c$  is the Henry's law constant ( $\text{J mol}^{-1}$ ),  $k_g$  is the gas-film mass transfer-coefficient ( $\text{cm s}^{-1}$ ), and  $k_s$  is the mass-transport coefficient at the surfactant film. The major problem with this approach is that it is difficult to measure or estimate the mass-transfer coefficients,  $k_g$ ,  $k_1$ , and  $k_s$ . However, for high volatility chemicals (high  $H_c$  values), such as ethanol and 1,1,1-trichloroethane studied in the present work, mass transfer in the liquid phase controls about 95% of the volatilization rate constant and, thus, the last term of Eq. 8 can be omitted.

### Evaporation under the influence of liquid free surface area

Tables 1 and 2 summarize the results obtained for ethanol and 1,1,1-trichloroethane, respectively, performing evaporation experiments under four different free surface areas of liquid, at 306.2 K.

The uncertainty of the used methodology is determined from the standard errors of  $k_c$  and  $D$  values estimated from the slopes of the linear plots of Eqs. 6 and 7, respectively. In the same tables, the values of diffusion coefficients found in the present work,  $D_{\text{found}}$ , and the corresponding literature values,  $D_{\text{lit}}$ , either calculated by using the Fuller-Schettler-Giddings equation<sup>25</sup> or experimentally obtained for the diffusivity of ethanol vapors in nitrogen, are also given.<sup>27</sup> The accuracy of the method is determined as % deviation of the experimental values,  $D_{\text{found}}$ , obtained by means of RF-GC, from the respective literature ones,  $D_{\text{lit}}$ .

$$\% \text{Deviation} = 100 \times \frac{|D_{\text{found}} - D_{\text{lit}}|}{D_{\text{lit}}} \quad (9)$$

The continuous elution GC method in a packed column was used for the determination of the experimental value for the

**Table 2. Rate Coefficients for the Evaporation of 1,1,1-Trichloroethane,  $k_c$ , and Diffusion Coefficients of Its Vapors Into Nitrogen,  $D_{\text{found}}$ , Under the Effect of Liquid Free Surface Area,  $a_L$ , at 306.2 K and 101325 Pa**

Vessel No	$10^5 a_L/\text{m}^2$	$10^5 k_c/\text{m s}^{-1}$	$10^5 D_{\text{found}}/\text{m}^2\text{s}^{-1}$	$10^5 D_{\text{lit}}/\text{m}^2\text{s}^{-1}$	Deviation, %
1	0.613	$9.67 \pm 0.07^a$	$0.92 \pm 0.004^a$	$0.87^\dagger$	$5.7^\dagger$
2	2.333	$9.71 \pm 0.05^a$	$0.90 \pm 0.007^a$	$0.87^\dagger$	$3.4^\dagger$
3	4.250	$10.0 \pm 0.11^a$	$0.92 \pm 0.005^a$	$0.87^\dagger$	$5.7^\dagger$
4	4.677	$10.3 \pm 0.09^a$	$0.91 \pm 0.006^a$	$0.87^\dagger$	$4.6^\dagger$
	Mean values		$0.91 \pm 0.005$		$(4.9^\dagger)^{**}$
	Precision, %		99.5*		

<sup>a</sup>Uncertainty obtained from the standard errors of the  $k_c$  and  $D$  values, estimated from the slopes of the linear plots of Eqs. 6 and 7, respectively.

\*Precision determined from the mean value and the standard error of the experimentally obtained diffusion coefficients.

\*\*Mean deviation of the experimental diffusion coefficients from the respective predicted<sup>†</sup> literature values,  $D_{\text{lit}}$ .

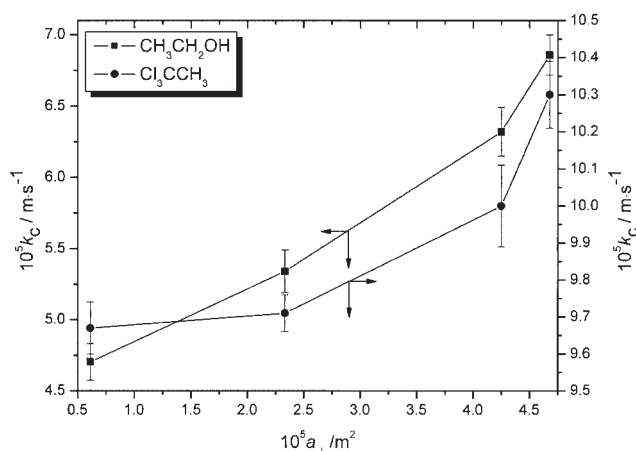


**Figure 5. Variation of the rate,  $k_c$ , for the evaporation of ethanol (■) and 1,1,1-trichloroethane (●), at various liquid free surface areas, at 306.2 K and 101325 Pa.**

diffusion coefficient of ethanol in nitrogen.<sup>27</sup> The calculation of the diffusion coefficient was based on the van Deemter equation at low carrier gas flow rates while the accuracy of the  $D$  value was 2.8%.<sup>28</sup>

From the results given in Tables 1 and 2, the following conclusions can be drawn.

From the experimentally found diffusion coefficients, the precision determined was 99.5%. The precision of other chromatographic methods used for the determination of diffusion coefficients, such as the continuous elution method, is about 98%, while that of the arrested-elution technique is also about 98%.<sup>23</sup> Hence, the present methodology compares satisfactorily with the other GC techniques.

The accuracy of the technique was checked by using the ethanol-nitrogen system, for which literature values predicted from the Fuller-Schettler-Giddings equation<sup>25</sup> as well as experimental ones obtained from the continuous elution GC method<sup>27</sup> are available. The comparison shows that the experimental results obtained by means of RF-GC differ from the respective literature in mean value by 3.8% and fall between predicted and experimental literature values. The mean percent deviation of the experimental values from the respective predicted ones is much smaller, 0.6%.

The uncertainty of the experimental,  $D_{\text{found}}$ , values, is less than 1.0%, ascertaining the reliability of the methodology. On

the other hand, the uncertainty of the experimental,  $k_c$ , values is between 1.8 and 2.8%, which is slightly larger than that of the  $D$  values. However, their uncertainty is satisfactory compared to that of other techniques; for example, the uncertainty in the measured evaporation rates by using a gravimetric technique varies from 1-4%.<sup>7</sup>

The variation of the experimentally obtained  $k_c$  values under the effect of the evaporating liquid free surface area is shown in Figure 5. At the smaller studied liquid surface area of  $0.613 \cdot 10^{-5} m^2$ ,  $k_c$  values differ by a factor of  $\sim$ two. At higher liquid surface areas, the evaporation rates of the two different studied liquids increase but their deviation decreases. Furthermore, it is obvious that in the studied liquid surface area range, the rate of 1,1,1-trichloroethane vaporization is always higher than that of ethanol but its increase is shorter than that of ethanol. For high volatility liquids substances such as those used in the present work, in the absence of surfactant layer(s), Eq. 8 predicts that the rate of vaporization is proportional to the interfacial area,  $a_L$ , and the liquid-film mass transfer coefficient,  $k_L$ . Bearing in mind that the change of surface area only affects  $a_L$ , the increase of  $k_c$  value is reasonable. Consequently, the more the free surface area of the liquid, the more molecules of liquid find their way to evaporate, in agreement with the predictions of the two-film theory for the evaporation. The values of  $k_c$  show bigger increase in the case of ethanol compared to 1,1,1-trichloroethane (Tables 1 and 2). This can be attributed to the different nature of each liquid, and it further indicates that additional complications may be taken into account.

### Evaporation under the influence of surfactant layers

Various resistances or barriers contribute in the evaporation rate. Commonly, the major resistance arises from the presence of "stagnant" gaseous and liquid layers close to the surface across which the vapor must diffuse. Additional resistance to evaporation, resulting in the drastic retardation of the evaporation rate, is caused by the presence of adsorbed monolayers.

Tables 3 and 4 summarize the results obtained for the evaporation of ethanol and 1,1,1-trichloroethane under the influence of various amounts of the nonionic surfactant Triton X-100, respectively. In the same tables, the diffusion coefficients experimentally determined,  $D_{\text{found}}$ , are compared with predicted ones from the Fuller-Schettler-Giddings equation<sup>25</sup> for ethanol and for 1,1,1-trichloroethane and with experimentally obtained values for the diffusion of ethanol in nitrogen.<sup>27</sup> In the last column of the tables, the deviation of the experimental values

**Table 3. Rate Coefficients for the Evaporation of Ethanol,  $k_c$ , and Diffusion Coefficients of Its Vapors Into Nitrogen,  $D_{\text{found}}$ , Under the Effect of Various Amounts of Surfactant Triton X-100, at 306.2 K and 101325 Pa**

Monolayer Thickness of Triton X-100	$10^5 k_c / m s^{-1}$	Retardation of $k_c$ , %	$10^5 D_{\text{found}} / m^2 s^{-1}$	$10^5 D_{\text{lit}} / m^2 s^{-1}$	$10^5 D_{\text{lit}} / m^2 s^{-1}$	Deviation, %	Deviation, %
0	$6.32 \pm 0.12^a$	—	$1.32 \pm 0.009^a$	$1.32^\dagger$	$1.37^\ddagger$	0 <sup>†</sup>	3.6 <sup>‡</sup>
1	$6.22 \pm 0.14^a$	1.6	$1.34 \pm 0.011^a$	$1.32^\dagger$	$1.37^\ddagger$	1.5 <sup>†</sup>	2.2 <sup>‡</sup>
2	$5.19 \pm 0.10^a$	17.9	$1.33 \pm 0.007^a$	$1.32^\dagger$	$1.37^\ddagger$	0.8 <sup>†</sup>	2.9 <sup>‡</sup>
3	$3.33 \pm 0.13^a$	47.3	$1.32 \pm 0.010^a$	$1.32^\dagger$	$1.37^\ddagger$	0 <sup>†</sup>	3.6 <sup>‡</sup>
4	$2.65 \pm 0.15^a$	58.1	$1.31 \pm 0.008^a$	$1.32^\dagger$	$1.37^\ddagger$	0.8 <sup>†</sup>	4.4 <sup>‡</sup>
Mean values			$1.32 \pm 0.005$			(0.6 <sup>†</sup> )**	(3.4 <sup>‡</sup> )**
Precision, %			99.6*				

<sup>a</sup>Uncertainty obtained from the standard errors of the  $k_c$  and  $D$  values, estimated from the slopes of the linear plots of Eqs. 6 and 7, respectively.

\*Precision determined from the mean value and the standard error of the experimentally obtained diffusion coefficients.

\*\*Mean deviation of the experimental diffusion coefficients from the respective predicted<sup>†</sup> and experimental<sup>‡</sup> literature values,  $D_{\text{lit}}$ .

**Table 4. Rate Coefficients for the Evaporation of 1,1,1-Trichloroethane,  $k_c$ , and Diffusion Coefficients of Its Vapors Into Nitrogen,  $D_{\text{found}}$ , Under the Effect of Various Amounts of Surfactant Triton X-100, at 306.2 K and 101325 Pa**

Monolayer thickness of Triton X-100	$10^5 k_c / \text{m s}^{-1}$	Retardation of $k_c$ , %	$10^5 D_{\text{found}} / \text{m}^2 \text{s}^{-1}$	$10^5 D_{\text{lit}} / \text{m}^2 \text{s}^{-1}$	Deviation, %
0	$10 \pm 0.11^a$	—	$0.92 \pm 0.009^a$	$0.87^\dagger$	$5.7^\dagger$
1	$9.70 \pm 0.14^a$	3.1	$0.92 \pm 0.007^a$	$0.87^\dagger$	$5.7^\dagger$
2	$9.50 \pm 0.12^a$	5.1	$0.91 \pm 0.005^a$	$0.87^\dagger$	$4.6^\dagger$
3	$9.30 \pm 0.16^a$	6.9	$0.93 \pm 0.006^a$	$0.87^\dagger$	$6.9^\dagger$
4	$7.30 \pm 0.13^a$	26.9	$0.92 \pm 0.008^a$	$0.87^\dagger$	$5.7^\dagger$
Mean values			$0.92 \pm 0.003$		$(5.8^\dagger)^{**}$
Precision, %			99.7*		

<sup>a</sup>Uncertainty obtained from the standard errors of the  $k_c$  and  $D$  values, estimated from the slopes of the linear plots of Eqs. 6 and 7, respectively.

\*Precision determined from the mean value and the standard error of the experimentally obtained diffusion coefficients.

\*\*Mean deviation of the experimental diffusion coefficients from the respective predicted<sup>†</sup> literature values,  $D_{\text{lit}}$ .

from the predicted and experimental literature values,  $D_{\text{lit}}$ , is given.

The values of the diffusion coefficients,  $D_{\text{found}}$ , show that they are independent of the addition of surfactant, as is expected. In the case of ethanol, the mean deviation of the experimentally obtained by means of RF-GC values,  $D_{\text{found}}$ , from the respective predicted and experimental literature ones is 0.6 and 3.4%, respectively.  $D_{\text{found}}$  values fall between predicted and experimental literature ones. In the case of 1,1,1-trichloroethane, the mean deviation of the experimental  $D_{\text{found}}$  values from the predicted ones is 5.5%. From the experimentally obtained diffusion coefficients,  $D_{\text{found}}$ , both under various liquid free surface areas and in the presence of surfactant, the total reproducibility of the method is determined 99.6% in the case of ethanol and 99.7% in the case of 1,1,1-trichloroethane.

The variation of the evaporation rates of ethanol and 1,1,1-trichloroethane in the presence of surfactant against the surface coverage of Triton X-100 is shown in Figure 6. The reduction of the evaporation rates of both solvents is presented in Figure 7.

The uncertainty in the determination of the vaporization values,  $k_c$ , varies from 2.7 to 5.7% in the case of ethanol, and from 2.2 to 3.6% in the case of 1,1,1-trichloroethane. Consequently, the experimentally obtained by means of RF-GC rates

can be used in order to extract safe conclusions for the effect of Triton X-100 in the evaporation of the studied solvents.

A general conclusion concerning the  $k_c$  values in the presence of various amounts of Triton X-100, corresponding to the formation of adsorbed monolayers at the liquid surface, is that the evaporation rates decrease. However, the reduction of the  $k_c$  values is different at each studied liquid. The retardation of the evaporation rate of ethanol becomes significant (>18%) at amounts of surfactant corresponding to more than two monolayers. Then, the  $k_c$  values decrease decently from 18 to 58% as the amount of Triton X-100 further increases. In the case of 1,1,1-trichloroethane, the reduction of  $k_c$  is obviously more slight. A small retardation of the vaporization rate of 1,1,1-trichloroethane, varying from 3 to 7%, is observed at coverages of surfactant corresponding from 1 to 3 theoretical monolayers. A higher amount of Triton X-100 is necessary for the drastic reduction (27%) of the vaporization rate of 1,1,1-trichloroethane.

The experimentally obtained evaporation rates are absolute and not relative ones and, consequently, they can be related to the physical properties of the evaporating species. They have units of velocity and, for high volatility compounds, their values are identified with the liquid film mass-transfer coefficients. They most likely indicate that the estimation of the cross

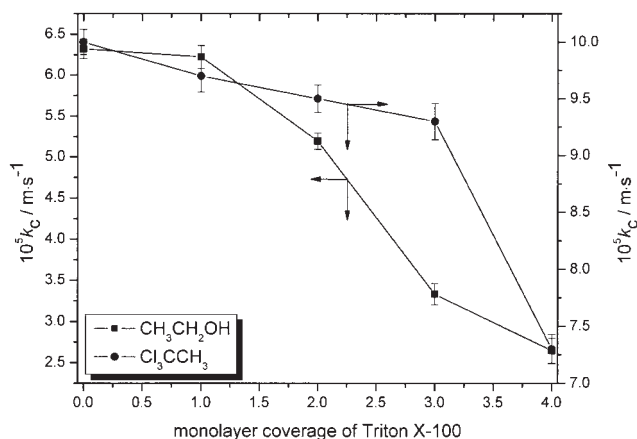


**Figure 6. Variation of the rate,  $k_c$ , for the evaporation of ethanol (■) and 1,1,1-trichloroethane (●), under the influence of various apparent surface coverages of surfactant Triton X-100, at 306.2 K and 101325 Pa.**

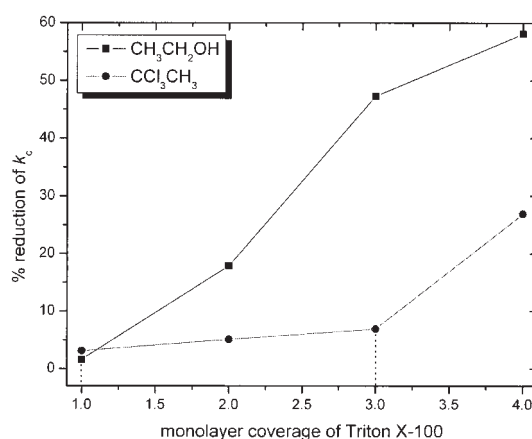


**Figure 7. Plots of the reduction (%) of the volatilization rate of ethanol (■) and 1,1,1-trichloroethane (●), under the influence of various apparent surface coverages of surfactant Triton X-100, at 306.2 K and 101325 Pa.**

sectional area,  $a_1^*$ , does not provide the necessary quantities of Triton X-100 required for the formation of the expected surfactant monolayers. In any case, it is obvious that higher amounts of surfactant than those predicted for the formation of a monolayer are necessary for the drastic reduction of the evaporation rate, which is in agreement with the observation that evaporation can be hindered only by very densely packed adsorption layers.<sup>14</sup>

Smith et al.<sup>8</sup> found that the addition of 0.003% v/v Triton X-100 results in reduction of the volatilization or evaporation rate of benzene at 20°C by a factor of 2. The retardation of the vaporization rate by Triton X-100 was attributed to the increase of the thickness of the boundary layer. Several workers have shown that surface active agents reduce the volatilization rate.<sup>13-18</sup> For example, Bull and Kamp<sup>15</sup> found a similar effect for the oxygen reaeration constant. Davies and Rideal<sup>16</sup> suggest that the presence of surfactant can also affect the liquid-film mass transfer coefficient,  $k_l$ , by increasing the viscosity of the surface. Similarly, Goodridge and Robb<sup>17</sup> found that amounts of  $C_{14}$  to  $C_{20}$  alcohols, corresponding to twice the amount required to form a monolayer, reduced the value of the evaporation rate constant by a factor of 1.5-4. In terms of classical two film theory, this is equivalent to an additional resistance, decreasing the value of liquid diffusivity,  $D_L$ , in the boundary layer. In terms of penetration or surface renewal theory, either  $D_L$  or the residence time of a packet at the surface can be reduced due to the surfactant monolayer(s).

The authors of a recent work examined by thermo-gravimetric balance the evaporation of water molecules across three kinds of interphases: (i) air/water, (ii) air/surfactant solution, and (iii) air/water interphase covered by an insoluble monolayer.<sup>29</sup> Their investigation of the first two interphases for three types of surfactant solutions below and above the critical micelle concentration showed that there was no difference in the evaporation rate of water, meaning that the molecular surface area from the Gibbs surface excess has nothing to do with the evaporation rate. In contrast, by using insoluble monolayers of 1-hetadecanol, the evaporation rate of water decreased, indicating a clear difference between an insoluble monolayer and an adsorbed film of soluble surfactant. The experimental findings of the present work may be explained in a similar way. The drastic reduction of the evaporation rate of ethanol and 1,1,1-trichloroethane at a coverage of 2 and 4 theoretical monolayers of Triton X-100, respectively, indicates that different amounts of surfactant, higher than those predicted from the Gibbs surface excess, are necessary for the formation of an insoluble monolayer.

It is also clear that the addition of Triton X-100 affects less the evaporation of 1,1,1-trichloroethane compared to that of ethanol. A similar behavior was also observed in the case of the effect of liquid surface area. This behavior can be related to the different nature of the two liquids. Both are polar compounds; however, ethanol is a protic solvent, which can stabilize both the surfactant cationic group through uncoupled electron pairs, as well as the anionic group through hydrogen bonds, probably ensuring a more favorable orientation of densely packed adsorption layers.

At nonionic surfactants, the surface-active portion bears no apparent ionic charge, and adsorbs onto surfaces with either the hydrophilic or the hydrophobic group oriented toward the surface, depending upon the nature of the surface. If polar

groups capable of H bonding with the hydrophilic group of the surfactant are present on the surface, such as in the case of ethanol, then the surfactant will probably be adsorbed with its hydrophilic group oriented toward the surface.<sup>20</sup> At low coverage, the nonionic surfactant molecule may lie prone on the surface, while at higher coverages, the hydrophobic group may be displaced from the surface by the hydrophilic group and lateral interactions between adjacent hydrophobic groups (hemimicelle formation) may occur.<sup>30</sup> Maximum adsorption, which occurs near the critical micelle concentration of the surfactant, has been ascribed to both monolayer and multilayer formation.<sup>30</sup> The present evaporation study, in the presence of Triton X-100, may indicate that maximum adsorption is associated with multilayer formation.

If polar groups capable of H bonding are absent from the surface, as in the case of 1,1,1-trichloroethane, then the non-ionic surfactant molecules will probably be oriented with their hydrophobic group toward the surface. The slight reduction of the evaporation rate of 1,1,1-trichloroethane, at coverage from 1 to 3 monolayers of Triton X-100, may be more indicative of micelle formation in the bulk than of monolayers at the solution/air interphase. Moroi et al.<sup>29</sup> also support that it seems quite fallacious to believe that the surface excess is concentrated at the air/solution interphase.

### Comparative study

A direct comparison of the measured in the present work  $k_c$  values with other literature ones is not possible. The majority of the literature volatilization rates are either evaporation half-times<sup>1,5,6</sup> or relative ones.<sup>8</sup> Dilling<sup>6</sup> measured evaporation rates of 27 chlorohydrocarbons from dilute water solutions (~1 ppm) and found the evaporation halftime of 1,1,1-trichloroethane to vary from 17.3 to 24.9 min depending on its initial aqueous concentration. Beverley et al.<sup>7</sup> measured the evaporation rate of ethanol equal to  $1.6 \text{ mg} \cdot \text{m}^{-1} \cdot \text{s}^{-1}$  at 298.2 K by a gravimetric technique. The latter value multiplied with the liquid free surface area,  $a_L$ , and divided by the mass of the evaporating liquid, which equals the product of ethanol volume,  $V$ , and its density,  $d$  ( $0.8 \text{ Kg} \cdot \text{m}^{-3}$ ), results in a value equal to  $1.6 \cdot 10^{-5} \text{ m} \cdot \text{s}^{-1}$ . This value is lower than the experimental value of our work:  $6.32 \cdot 10^{-5} \text{ m} \cdot \text{s}^{-1}$  at 306.2 K. Unfortunately, a proper comparison between the two values is not easy since they are not only referred to different temperatures but moreover the former has been measured by using a gravimetric technique depending on the gas flow rate while the latter, by RF-GC, which does not at all depend on the carrier gas flow rate. In any case, they are of similar order of magnitude.

Based on the vapor pressures and the boiling points of the two studied for their evaporation liquids as given by BDH chemicals (59 hPa and 351.2 K in the case of ethanol and 13.3 kPa and 347.2 K in the case of 1,1,1-trichloroethane), it is expected for 1,1,1-trichloroethane to be more volatile. This is exactly what is experimentally observed (Tables 1-4 and Figures 5 and 6), further validating the reliability of the present work. Additional complications may arise at high evaporation rates because evaporation leads to a cooling of the liquid surface with consequent reduction of the vapor pressure. In this situation, the evaporation rate is coupled to the rate of heat transfer in the surface region.<sup>7</sup>

The values of the experimentally determined vaporization



rates for high volatility compounds are identified with the liquid film mass-transfer coefficients (Eq. 8). Thus, the liquid film mass transfer coefficients,  $k_l$ , of ethanol and 1,1,1-trichloroethane at 306.2 K are estimated equal to  $6.32 \cdot 10^{-5}$  and  $10 \cdot 10^{-5} \text{ m}\cdot\text{s}^{-1}$ , respectively. The latter compare successfully to literature values of  $k_l$ , such as a value  $5.55 \cdot 10^{-5} \text{ m}\cdot\text{s}^{-1}$  given by Liss and Slater for  $\text{CO}_2$  in water,<sup>31</sup> further ascertaining the validity of the present work. The thickness of the liquid stagnant film,  $z_l$ , can be obtained from the ratio of the respective diffusion coefficient,  $D_L$ , divided by the mass transfer coefficient through the stagnant liquid film,  $k_l$ . Thus, the stagnant liquid layer thickness can be experimentally determined from the values of the self diffusion coefficient at 306.2 K (corresponding to the diffusion of ethanol vapors into ethanol), estimated from the semi-empirical equation of Wilke-Chang<sup>23</sup>:  $1.6 \cdot 10^{-9} \text{ m}^2\cdot\text{s}^{-1}$  for ethanol and  $2.9 \cdot 10^{-9} \text{ m}^2\cdot\text{s}^{-1}$  for 1,1,1-trichloroethane, and the experimentally known  $k_l$  values. These values are:  $2.6 \cdot 10^{-4} \text{ m}$  in the case of ethanol and  $5.9 \cdot 10^{-4} \text{ m}$  in the case of 1,1,1-trichloroethane. The latter values are very close to the respective literature value given by Liss and Slater<sup>31</sup> for the transfer of oxygen in water:  $4.0 \cdot 10^{-4} \text{ m}$ .

### Advantages of the present methodology

The basic advantage of the technique is its precision and experimental simplicity. Absolute evaporation rates, which are independent of the carrier gas flow-rate and, furthermore, related to the physical properties of the evaporating liquids, are determined simultaneously with the respective diffusion coefficients of the evaporating vapors into the carrier gas. The experimentally determined vaporization rates have units of velocity and, for high volatility compounds, their values are identified with the liquid film mass-transfer coefficients (Eq. 8), which measurement or estimation is considered as a difficult task in the literature.<sup>8</sup> The validity of the method lies also in the fact that it yields the above parameters not only for pure liquids but also for their solutions.

### Conclusions

The presented methodology of reversed-flow gas chromatography can be used to simultaneously determine accurate absolute evaporation rates and vapors diffusivities of pure liquids, precisely.

The use of RF-GC can be obviously extended in topics that are related to processes of significant environmental interest, such as: (i) Studies from dilute aqueous solutions of organic and inorganic pollutant compounds; (ii) Investigation of water evaporation (sea, lake, river water bodies); (iii) Effect of ionic and zwitterionic surfactants; (iv) Experiments with a longer duration (>1 day) in order to examine the change of the evaporation rate in a broader time scale (determination of evaporation rates at a time resolved procedure) and, moreover, the life span of the studied surfactant; and (v) Experiments with surfactants under steering conditions in order to investigate their durability. In a future publication, experimental results concerning evaporation studies from dilute aqueous solutions of organic pollutant compounds are going to be presented.

### Literature Cited

1. Dilling WL, Tefertiller NB, Kallos G. Evaporation rates and reactivities of methylene chloride, chloroform, 1,1,1-trichloroethane, trichloroethylene, tetrachloroethylene, and other chlorinated compounds in dilute aqueous solutions. *Environ Sci Technol.* 1975;9: 833-838.
2. Hill J IV, Kollig HP, Paris DF, Wolfe NL, Zepp RG. Dynamic behavior of vinyl chloride in aquatic ecosystems. U.S. Environ Prot Agency, Off. Res. Dev. Rept. No. EPA-600/3-76-001; 1976:64.
3. Acree F, Beroza M, Bowman MC. Codistillation of DDT with water. *J Agric Food Chem.* 1963;11:278-280.
4. Mackay D, Wolkoff WA. Rate of evaporation of low solubility contaminants from water bodies to atmosphere. *Environ Sci Technol.* 1973;7:611-614.
5. Mackay D, Leinonen P. Rate of evaporation of low solubility contaminants from water bodies to atmosphere. *Environ Sci Technol.* 1975; 9:1178-1180.
6. Dilling WL. Interphase transfer processes. II. Evaporation rates of chloro methanes, ethanes, ethylenes, propanes, and propylenes from dilute aqueous solutions: comparisons with theoretical predictions. *Environ Sci Technol.* 1977;11:405-409.
7. Beverley KJ, Clint JH, Fletcher PDI. Evaporation rates of pure liquids measured using a gravimetric technique. *Phys Chem Chem Phys.* 1999;1:149-153.
8. Smith JH, Bomberger Jr DC, Haynes DL. Prediction of the volatilization rates of high-volatility chemicals from natural water bodies. *Environ Sci Technol.* 1980;14:1332-1337.
9. Karaiskakis G, Katsanos NA. Rate coefficients for evaporation of pure liquids and diffusion coefficients of vapors. *J Phys Chem.* 1984;88: 3674-3678.
10. Karaiskakis G, Agathonos P, Niotis A, Katsanos NA. Measurement of mass transfer coefficients for the evaporation of liquids by reversed-flow gas chromatography. *J Chromatogr.* 1986;364:79-85.
11. Agathonos P, Karaiskakis G. Measurement of activity coefficients, mass-transfer coefficients and diffusion coefficients in multicomponent liquid mixtures by reversed-flow gas chromatography. *J Chem Soc Faraday Trans.* 1989;85(6):1357-1363.
12. Koliadima A, Agathonos P, Karaiskakis G. Estimation of solubility and interaction parameters in binary liquid mixtures by reversed-flow gas chromatography. *Chromatographia.* 1988;26: 29-33.
13. LaMer VK, Healy TW. Evaporation of water: its retardation by monolayers. *Science.* 1965;148:36-42.
14. Lunkenheimer K, Zembala M. Attempts to study a water evaporation retardation by soluble surfactants. *J Colloid & Interf Sci.* 1997;188: 363-371.
15. Bull DN, Kempe LL. Influence of surface active agents on oxygen absorption to the free interface in a stirred fermentor. *Biotechnol Bioeng.* 1971;13:529-547.
16. Davies JT, Rideal EK. *Interfacial Phenomena.* New York: Academic Press; 1961.
17. Goodridge F, Robb ID. Mechanism of interfacial resistance in gas absorption. *Ind Eng Chem Fundam.* 1965;4:49-55.
18. Barnes GT. The effects of monolayers on the evaporation of liquids. *Adv Colloid & Inter Sci.* 1986;25: 89-200 (Review).
19. Hsin Y-LL. *Feasibility Experiments into the Use of Hexadecanol for Hurricane Mitigation and the Planning and Construction of the Monolayer Evaporation Retardation.* Bachelor Degree Thesis, Massachusetts Institute of Technology, June 2002.
20. Rosen MJ. *Surfactants and Interfacial Phenomena.* New York: John Wiley & Sons; 1989:67-68.
21. Rashid KA, Gavril D, Katsanos NA, Karaiskakis G. Flux of gases across the air-water interface studied by reversed-flow gas chromatography. *J Chromatogr A.* 2001;934:31-49.
22. Atta KR, Gavril D, Loukopoulou V, Karaiskakis G. Study of the influence of surfactants on the transfer of gases into liquids by inverse gas chromatography. *J Chromatogr A.* 2004;1023:287-296.
23. Karaiskakis G, Gavril D. Determination of diffusion coefficients by gas chromatography. *J Chromatogr A.* 2004;1037: 147-189 (Review).
24. Bird RB, Stewart WE, Lightfoot EN. *Transport Phenomena.* New York: John Wiley & Sons; 1960:511.
25. Fuller EN, Shettler PD, Giddings JC. A new method for prediction of binary gas-phase diffusion coefficients. *Ind Eng Chem.* 1966;58: 18-27.

26. Whitman WG. Preliminary experimental confirmation of the two-film theory of gas absorption. *Chem Metall Eng.* 1923;29:146-148.
27. Arnkar HJ, Ghule HM. Electrodeless discharge as detector in the rapid determination of binary diffusion coefficient of gases. *Int J Electronics.* 1969;26:159-162.
28. Maynard VR, Grushka E. Measurement of diffusion coefficients by gas chromatography broadening techniques: A review. *Adv Chromatogr.* 1975;12:99-140.
29. Moroi Y, Rusdi M, Kubo I. Difference in surface properties between insoluble monolayer and adsorbed film from kinetics of water evaporation and BAM image. *J Phys Chem B.* 2004;108:6351-6358.
30. Partyka S, Zaini S, Lindheimer M, Brun B. Adsorption of non-ionic surfactants on a silica gel. *Colloids Surf.* 1984;12:255-270.
31. Liss PS, Slater PG. Flux of gases across the air-sea interface. *Nature (London).* 1974;247:181-184.

*Manuscript received Oct. 18, 2005, and revision received Mar. 14, 2006.*